

## Analysis on the Triaxial Loading Mechanical Properties of Sandstone under High Stress and High Hydraulic Pressure

Jun Liu<sup>1, 2, 3</sup>, Xinrong Liu<sup>2\*</sup>, Chuan He<sup>1</sup>, Kaishun Zhang<sup>3</sup>, Zusong Wu<sup>4</sup> and Bin Zeng<sup>5</sup>

<sup>1</sup>School of Civil Engineering, Southwest Jiaotong University, Chengdu, Sichuan 610031, China

<sup>2</sup>Key Laboratory of New Technology for Construction of Cities in Mountain Area (Chongqing University), Ministry of Education, Chongqing 400030, China

<sup>3</sup>The 5th Engineering Co., Ltd of China Railway 11th Bureau Group, Chongqing 400037, China

<sup>4</sup>International College, Chongqing Jiaotong University, Chongqing, 400074, China

<sup>5</sup>School of Civil, Environmental and Mining Engineering, The University of Western Australia, Crawley; WA; 6009, Australia

Received 17 February 2019; Accepted 29 May 2019

### Abstract

The mechanical properties of deep rocks are highly sensitive to hydraulic pressures. The existing associated studies mainly focused on the mechanical properties of rocks under high stress, but few studies analyzed the collaborative influences of high stress and high hydraulic pressure on deep rocks. To analyze the special mechanical properties of deep rocks under high hydraulic pressure, sandstone samples were collected from a deep tunnel of the Yuanliangshan Line in Chongqing, China. All rock samples were saturated in vacuum conditions and then wrapped with oil in a specially made fluororubber cover. Then the confining pressure was loaded to 15, 25, 35, and 45 MPa at a loading rate of 1 MPa/min under hydrostatic pressure conditions. After reaching the preset confining pressure, the rock samples were resaturated in the experimental apparatus. The outlet pressure was maintained at a barometric pressure, while the inlet pressure was the preset hydraulic pressures of 1, 4, and 7 MPa, thus forming a one-way interstitial flow. A triaxial compression test was performed on the sandstone samples under high stress and high hydraulic pressure. Results demonstrate that under high stress, the compressive strength of sandstone decreases in the logarithmic function along with an increasing hydraulic pressure ( $p$ ). A regression analysis was performed on the elasticity modulus of sandstone with an increasing confining pressure ( $\sigma_3$ ) and under different hydraulic pressures. Under different confining pressures, the elasticity modulus of sandstone decreases in logarithmic function along with an increasing hydraulic pressure. Meanwhile, under an increasing confining pressure, the sandstone samples shift from a brittle state to a ductile state. However, the brittleness of these samples is positively related with hydraulic pressure. The findings of this work provide references for analyzing the excavation-induced mechanical properties of deep rocks in tunnels under high hydraulic pressure.

**Keywords:** high stress, high hydraulic pressure, mechanical properties, triaxial compression test, elasticity modulus.

### 1. Introduction

Given the extensive construction of highways, railways, and large hydropower engineering structures in China as well as the large-scale deep exploitation of coal mine resources, the number of deep rock engineering problems under high hydraulic pressures continues to increase. Therefore, maintaining the stability of rock mass in deep underground tunnels under high stress poses a great challenge in engineering construction in China. For example, the excavation and construction of diversion tunnels at the Laxiwa and Jinping Hydropower Stations involve high stress and high hydraulic pressure. The second-level diversion tunnel in Jinping Station is buried at a depth of 1500 m to 2000 m, a maximum measured geostress of 42.1 MPa, and a maximum hydraulic pressure of 10.2 MPa.

Deep brittle rocks under high geostress show significantly different deformation failure characteristics and mechanisms compared with those rocks under ordinary stress. Previous studies [1-3] have mainly focused on

following aspects: (1) rocks are suddenly peeled or shot off when under high stress due to the sudden release of energy as manifested in their brittle failure; and (2) due to the failure complexity of deep brittle rocks, the excavation of deep tunnels may change the major control effect over rock strength. These studies have also analyzed the mechanical properties of rocks mainly under single factor conditions, including their pore water pressure, temperature, or stress, while few of them have examined the coupling effect of multiple factors, especially the coupling effect between stress and pore water pressure. Therefore, these studies are unable to determine the mechanical properties of rock mass under high stress and high hydraulic pressure.

This study performs a triaxial compression test of sandstone under high stress and high hydraulic pressure to solve the mechanical problems faced in underground excavation projects when under high hydraulic pressures. In this test, the influences of confining and hydraulic pressures on the mechanical properties of sandstone were analyzed. The findings of this work provide some references for analyzing the excavation-induced mechanical properties of deep rocks in underground tunnels under high hydraulic pressures.

\*E-mail address: liuxrong@126.com

ISSN: 1791-2377 © 2019 School of Science, IHU. All rights reserved.

doi:10.25103/jestr.124.14

## 2. State of the art

Basic mechanical properties or rock mass can be tested through a triaxial compression test. Previous studies mainly concentrate on mechanical properties of rock mass under different pore water pressures, temperatures, confining pressure or different strain rates.

Yang [4] studied mechanical properties of red sandstone under different pore water pressures by using the servo control triaxial equipments, concluding a positive correlation between peak strength of red sandstone and confining pressure. Meanwhile, influences of hydraulic pressure on mechanical properties of red sandstone were analyzed preliminarily. Alam [5] studied permeabilities of three different rock masses under 1-15MPa, finding significant differences of permeability of three different rock masses with the change of confining pressure. This study interpreted influences of confining pressure on mechanical properties of rocks to some extent. Hokka [6,7] carried out a systematic study on mechanical properties of Kuru Gray granite under strain rates of  $10^{-6} \text{ s}^{-1}$  and  $600 \text{ s}^{-1}$ . With the increase of strain rate and confining pressure, rock strength was increased significantly and material strength increased more quickly under high strain when there's a limit of below 20MPa. When the pressure is higher than 20MPa and there's a low strain, confining pressure influence mechanical properties of rock mass more significantly. Tkalich [8] carried out a triaxial compression test of Kuru Gray granite under different confining pressure levels. He pointed out that the peak pressure under the confining pressure of 150MPa was increased by about 11% compared with that under no lateral confinement and shape of the equivalent stress field close to the free face of rocks was sensitive to confining pressure. Although he analyzed mechanical properties of rock samples under high confining pressure, influences of pore water pressure were not investigated. Sakai [9-11] performed a triaxial test of cement paste under high pressure, finding that the deviator stress-axial strain relation is unrelated with confining pressure during the plastic deformation when the confining pressure is higher than 30MPa. This research conclusion provided some references to study mechanical properties of deeply buried concrete structures. In addition, mechanical properties of cement paste under high stress could be gained if it is viewed as a kind of rock material. To study mechanical and permeability characteristics of rock mass under full stress-strain conditions, Zhao [12-13] carried out an experimental study on fractured limestone and found that describing permeability and volume strain in the volume compression stage by using the cubic polynomial can improve mechanical characteristic laws of rock samples under high stress and high hydraulic pressures to some extent. However, further deep studies are still needed. These studies mainly focus on mechanical properties under single-factor conditions, such as pore water pressure, confining pressure or loading rate. Since more and more underground projects are launched, rock mass faces with various complicated environment, such as coupling effect of pore water pressure, temperature and high stress. Among them, influences of water are extremely prominent. Therefore, underground excavation projects under high stress and high hydraulic pressure, that is, coupling effect of confining pressure and pore water pressure, appear gradually. Now, there are few studies on mechanical properties of rock mass under coupling effect.

Chernak et al. [14-18] studied mechanical properties of rock mass under high temperature, finding that the change

rate of permeability was different under different temperatures. Given the high confining pressure, temperature influenced permeability slightly. Additionally, the coupling effect of temperature and confining pressure on mechanical properties of rock sample was analyzed, which could provide references to multi-factor analysis on mechanical properties of rock samples. To solve problems in deep underground project under high hydraulic pressure, existing associate studies on mechanical properties of rock mass under the collaborative effect of high stress and high hydraulic pressure are small in quantity [19] and superficial. However, more and more underground projects will face with collaborative effects of high stress and high hydraulic pressure. In other words, peak strength, residual strength and elasticity modulus of rock mass under high stress and high hydraulic pressure have to be analyzed in the same time for the convenience of engineering excavation. Hence, it is extremely urgent and important to investigate mechanical properties of rocks under the coupling effect of high stress and high hydraulic pressure.

As a result, a triaxial compression test of sandstone under high stress and high hydraulic pressure was carried out in this study. Hydraulic pressure was set 1, 4 and 7 MPa, while the confining pressure was set 15, 25, 35 and 45MPa, respectively. Variation laws of mechanical properties of rocks under different stresses and hydraulic pressures were analyzed. Research conclusions provide some practical theoretical references for excavation of deep underground projects under high hydraulic pressures, aiming to provide references for similar projects in future.

The rest of the study is organized as follows. Section 3 introduces the material, equipment and method of the test. Section 4 describes the strength and deformation characteristics of the specimens, and finally, the conclusions are summarized in Section 5.

## 3. Methodology

### 3.1 Experiment

#### 3.1.1 Rock samples

The rock samples used in this study were sandstone collected from the deep tunnel of the Yuanliangshan Line in Chongqing, China. According to the results of the thin section authentication, these sandstone samples were identified as glaucous middle-thin arkose based on their porous cementation. The mineral content of these samples is presented in Table 1. These samples were processed into cylinder samples with a 2:1 height-diameter ratio (diameter  $D=50 \text{ mm}$  and height  $H=100 \text{ mm}$ ).

**Table 1.** Mineral content of sandstone samples

Rock debris (96%)				Interstitial materials (4%)	Heavy minerals	
Qua -rtz 50%	Feld- spar 40%	Rock debris 5%	Mica 1%	Clay (chlorite) 4%	Almand -ine Occasio -nally	Zircon Occasio -nally

#### 3.1.2 Experimental apparatus

The triaxial test was accomplished using the “multi-field coupling triaxial apparatus of rocks” in the Geotechnical Laboratory Building of District B, Chongqing University. This apparatus was developed by USTL, France and manufactured by Top Industrie. The experimental apparatus is shown in Fig. 1.



**Fig. 1.** Experimental apparatus and sandstone samples

### 3.2 Test method

Based on the stress and hydraulic pressure of the sandstone samples, the hydraulic pressure was set to 1, 4, and 7 MPa, while the confining pressure was set to 15, 25, 35, and 45 MPa (when the vertical stress is 15 MPa, the buried depth can be calculated at about 553.5 m. The hydraulic pressure of 7 MPa was unavailable under this confining pressure. Therefore, the hydraulic pressure was set between 1 MPa and 4 MPa when the confining pressure was 15 MPa). The test steps are explained as follows:

Step 1: All sandstone samples were saturated under vacuum conditions and wrapped with oil in a specially made fluororubber cover to prevent the hydraulic oil from infiltrating the rock samples during the test process and influencing the parameter test results. These samples were packed and then compressed into the confining pressure chamber. The confining pressure was increased to the preset value (15, 25, 35 and 45 MPa) under hydrostatic pressure conditions at a loading rate of 1 MPa/min.

Step 2: After the confining pressure reached the preset value, the rock samples were re-saturated in the experimental apparatus. The outlet pressure was maintained at the barometric pressure, while the inlet pressure was the preset hydraulic pressure (1, 4, and 7 MPa), thereby generating a one-way interstitial flow (in this process, the hydraulic pressure can be increased to one hydraulic value lower than the confining pressure to shorten the saturation time). The sandstone samples were filled with water until water was discharged from the outlet. This process lasted for 3 h to 8 h. The inlet end was set at the hydraulic pressure, while the outlet pressure was kept at the barometric pressure, that is, a hydraulic pressure of 0 MPa, thereby creating a hydraulic pressure gap. In this case, the hydraulic pressure was loaded to the sandstone samples. The loading system of the apparatus is shown in Fig. 2.

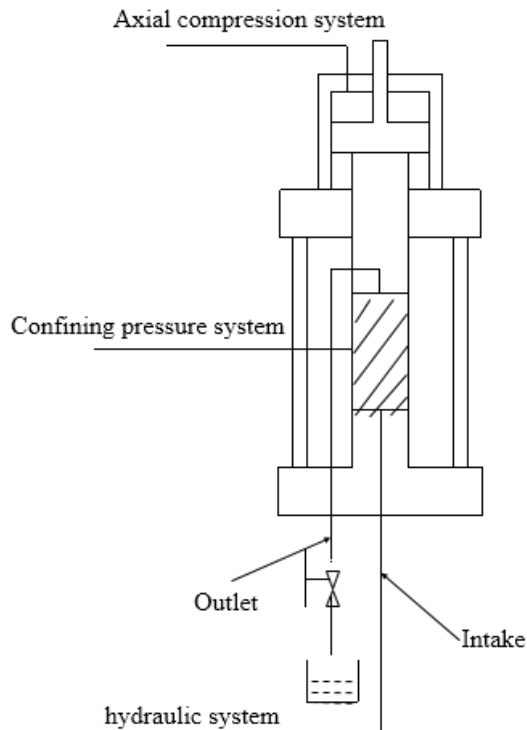


**Fig. 2.** Loading system of the multi-field coupling triaxial apparatus of rocks

Step 3: The axial loading continued until the sandstone samples entered the residual stage. The data acquisition process was stopped, and the hydraulic, axial, and confining pressures were relieved. The sandstone samples were then taken out of the experimental apparatus.

## 4. Result Analysis and Discussion

### 4.1 Strength characteristics

#### (1) Peak strength characteristics

Using the above test program, the strength of the sandstone samples under different high stresses and high hydraulic pressures was analyzed. The variations in their peak strength along with confining and hydraulic pressures are shown in Table 2.

**Table 2.** Compressive strength of the sandstone samples under different confining and hydraulic pressures

Confining pressure /MPa	Compressive strength of sandstone/MPa			
	Hydraulic pressure 0 MPa	Hydraulic pressure 1 MPa	Hydraulic pressure 4 MPa	Hydraulic pressure 7 MPa
15.0	100.5	93.5	90.0	--
25.0	127.3	122.2	115.4	108.3
35.0	145.4	140.1	135.1	128.1
45.0	160.9	155.2	148.6	142.8

Table 2 shows that

1) Under the same confining pressure, the peak strength of sandstone reaches the maximum under the hydraulic pressure of 0 MPa. This peak strength then gradually decreases along with a continuous increase in hydraulic pressure.

2) The peak strength of sandstone sharply decreases when the hydraulic pressure increases from 0 MPa to 1 MPa but slightly decreases when the hydraulic pressure increases

from 1 MPa to 7 MPa. When the confining pressure is 35 MPa and when the hydraulic pressure increases from 0 MPa to 1 MPa, the strength of the sandstone decreases by 5.3 MPa. The average reduction in strength (relative to its original state) is 3.65%. The strength of the sandstone samples decreases by 5.0 MPa (1.19%) when the hydraulic pressure increases from 1 MPa to 4 MPa and further decreases by 7.1 MPa (1.73%) when the hydraulic pressure increases from 4 MPa to 7 MPa. These trends indicate that the influences of hydraulic pressure on the strength of sandstone are gradually weakened possibly because some regions of the sandstone samples are not filled with water under a small hydraulic pressure. As the hydraulic pressure increases, all sandstone samples are filled of water, thereby guaranteeing the stable influences of hydraulic pressure. Similar laws are observed under other confining pressures.

3) Under the same hydraulic pressure, the peak strength of the sandstone samples under a high confining pressure shows a linear relationship with the initial confining pressure.

The compressive strength of sandstone is hypothesized to continuously change along with hydraulic pressure ( $p$ ). To check the variations of the curves, a regression analysis on the strength of the sandstone samples under different initial confining and hydraulic pressures was performed by using the logarithmic function. The data in Table 2 were fitted to obtain the trend presented in Fig. 3. The fitting expression is shown as follows:

$$\sigma_c(p) = \sigma_c^0 [1 - a \ln(p + 1)] \quad (1)$$

where  $\sigma_c(p)$  is the compressive strength when the hydraulic pressure is  $p$ ,  $\sigma_c^0$  is the compressive strength under the hydraulic pressure of 0 MPa, and  $a$  is the regression coefficient. The fitting results reveal that the fitting correlation coefficient exceeds 0.90 and that the fitting effect is relatively ideal.

When the confining pressure is 15 MPa, the fitting formula and correlation coefficient are

$$\sigma_c(p) = 100.5 [1 - 0.07275 \ln(p + 1)] R^2=0.90172 \quad (2)$$

When the confining pressure is 25 MPa, the fitting formula and correlation coefficient are

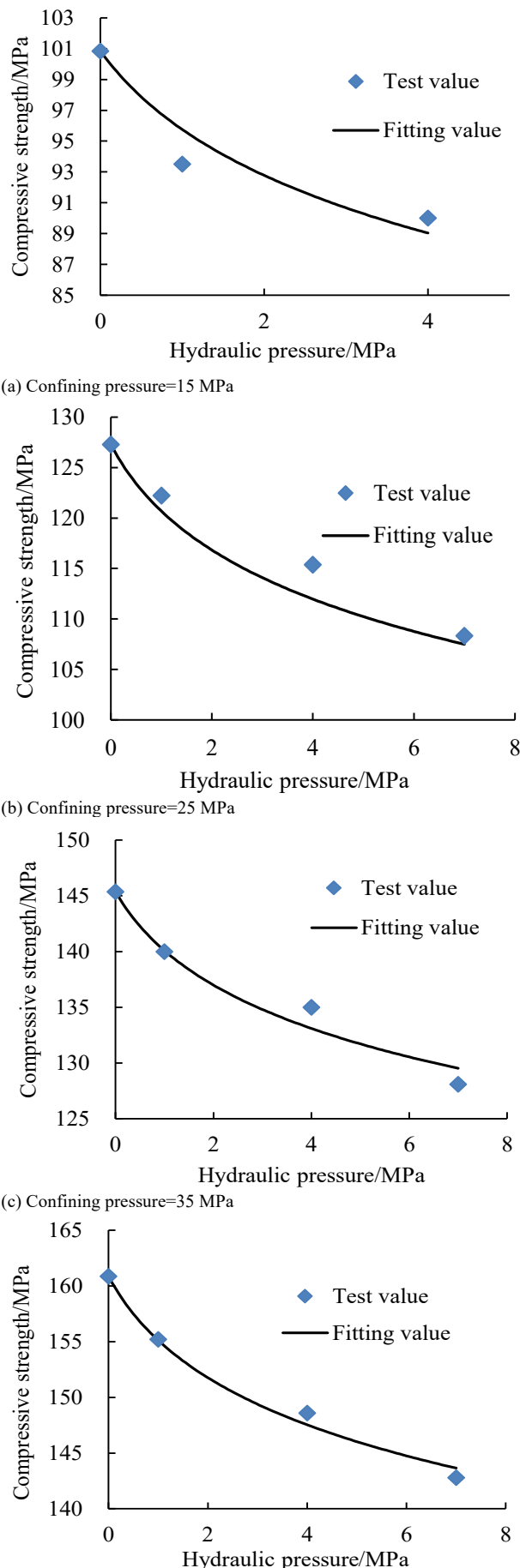
$$\sigma_c(p) = 127.3 [1 - 0.07477 \ln(p + 1)] R^2=0.91892 \quad (3)$$

When the confining pressure is 35 MPa, the fitting formula and correlation coefficient are

$$\sigma_c(p) = 145.4 [1 - 0.05239 \ln(p + 1)] R^2=0.96489 \quad (4)$$

When the confining pressure is 45 MPa, the fitting formula and correlation coefficient are:

$$\sigma_c(p) = 160.9 [1 - 0.05143 \ln(p + 1)] R^2=0.98994 \quad (5)$$



(d) Confining pressure=45 MPa

**Fig. 3.** Relation curves of the compressive strength of sandstones under different confining and hydraulic pressures ( $p$ )

The relationships of the compressive strength of sandstones with the confining and hydraulic pressures were then examined. The test data in Table 2 were fitted to identify the following binary functional relation among these three parameters:

$$\sigma_c = a\sigma_3 \ln(p+1) + b \ln(p+1) + c\sigma_3 + d \quad (6)$$

where  $\sigma_c$  is the compressive strength under different confining and hydraulic pressures,  $p$  is the hydraulic pressure,  $\sigma_3$  is confining pressure, and  $a$ ,  $b$ ,  $c$ , and  $d$  denote the regression parameters. The fitting surface is shown in Fig. 4, where  $a=-0.09578$ ,  $b=-4.593$ ,  $c=2.043$ , and  $d=72.11$ . The correlation coefficient ( $R^2$ ) is 0.9804. The functional relationships of the compressive strength of sandstone with the confining and hydraulic pressures are all reasonable. Moreover, the compressive strength under different confining and hydraulic pressures is predicted based on the values of  $\sigma_3$  and  $p$  in this binary function.

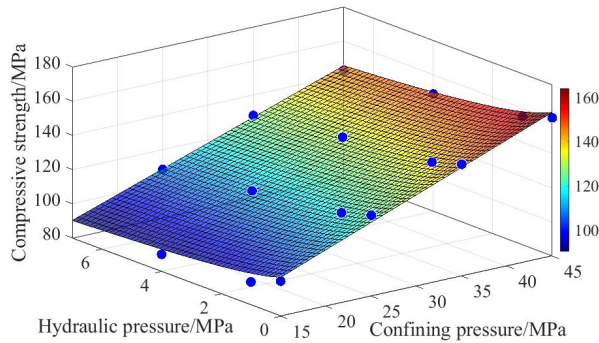


**Fig. 4.** Relationships of compressive strength with hydraulic ( $P$ ) and confining pressures ( $\sigma_3$ )

#### (2) Residual strength characteristics

The residual strength ( $\sigma_r$ ) of sandstone under different high stresses and high hydraulic pressures was then examined. The variations in residual strength with confining and hydraulic pressures are shown in Table 3.

**Table. 3.** Residual strength of sandstone under different confining and hydraulic pressures

Confining pressure /MPa	Residual strength of sandstone /MPa			
	Hydraulic pressure 0 MPa	Hydraulic pressure 1 MPa	Hydraulic pressure 4 MPa	Hydraulic pressure 7 MPa
15	48.2	39.5	28.7	--
25	75.0	67.5	59.0	44.9
35	95.0	89.5	80.5	69.4
45	115.6	110.6	107.2	104.1

Given the same hydraulic pressure, the residual strength linearly increases along with confining pressure. This trend follows the variation law of peak strength. Given the same confining pressure, the residual strength of sandstone gradually decreases along with an increasing hydraulic pressure, thereby indicating that the effective stress decreases due to hydraulic pressure and that the residual strength decreases accordingly. Given that the variation law of residual strength is similar to that of compressive strength, the binary functional relationships of axial peak strain (Table 3) with confining and hydraulic pressures are directly fitted.

The fitting relations are

$$\sigma_r = a\sigma_3 \ln(p+1) + b \ln(p+1) + c\sigma_3 + d \quad (7)$$

where  $\varepsilon_c$  is the axial peak strain under different confining and hydraulic pressures,  $p$  is the hydraulic pressure,  $\sigma_3$  is the confining pressure, and  $a$ ,  $b$ , and  $c$  are the regression parameters. The fitting surface is shown in Fig. 5, where  $a=0.2471$ ,  $b=-18.24$ ,  $c=2.202$ ,  $d=18.03$ , and  $R^2=0.9901$ . In sum, the functional relationships of the residual strength of sandstone with confining and hydraulic pressures are reasonable. In addition, the residual strength of sandstone under different confining and hydraulic pressures can be predicted based on the values of  $\sigma_3$  and  $p$  in this binary function.

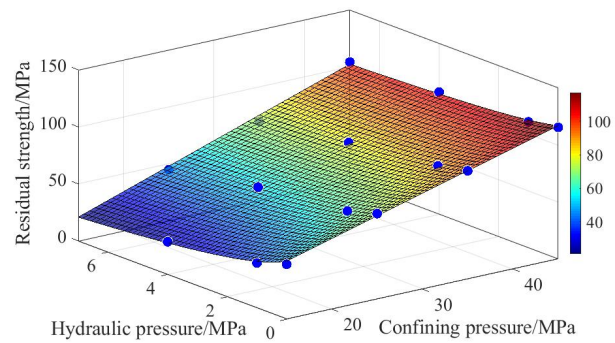


**Fig. 5.** Relationships of residual strength with hydraulic ( $P$ ) and confining pressures ( $\sigma_3$ )

#### 4.2 Deformation parameters

##### (1) Change characteristics of elasticity modulus

The elasticity modulus and Poisson's ratio of sandstone under different confining and hydraulic pressures can be obtained based on the previous empirical calculations. The Poisson's ratio is irregular and ranges between 0.213 and 0.284. Therefore, the Poisson's ratio was not analyzed in this study. The elasticity modulus of sandstone under different confining and hydraulic pressures was then analyzed. The results are shown in Table 4.

**Table. 4.** Elasticity modulus of sandstone under different confining and hydraulic pressures

Confining pressure /MPa	Elasticity modulus $E$ /GPa			
	Hydraulic pressure 0 MPa	Hydraulic pressure 1 MPa	Hydraulic pressure 4 MPa	Hydraulic pressure 7 MPa
15	15.4	14.5	13.9	--
25	16.5	15.8	14.7	13.4
35	17.3	16.2	15.6	14.2
45	17.6	16.5	15.8	14.9

Table 4 shows that

1) Given the same hydraulic pressure, the elasticity modulus is positively correlated with confining pressure. As the confining pressure linearly increases, the elasticity modulus fails to demonstrate a synchronous linear growth. Instead, the growth of the elasticity modulus decreases under a high confining pressure. Rock failure can be divided into five stages, of which three stages (pore compaction, elastic compression, and crack extension stages) occur before the peak strength is reached. At a low level, the confining pressure significantly affects both the initial porosity of sandstones and the elasticity modulus. Meanwhile, under a

high confining pressure, the initial pores in sandstones become compact and the confining effect of elasticity modulus decreases. The growth of the elasticity modulus of sandstone eventually declines along with an increasing confining pressure. The confining pressure increases from 15 MPa to 25 MPa when the hydraulic pressure is 3 MPa and when the confining pressure increases from 15 MPa to 25 MPa. The confining pressure further increases by 0.3 GPa when the confining pressure increases from 25 MPa to 35 MPa.

2) Under the same confining pressure, the elasticity modulus gradually decreases along with an increasing hydraulic pressure. In this test, the adhesion among the particles in sandstone samples is weakened by hydraulic pressure, which can easily lead to the dislocation of particles and a decrease in elasticity modulus. Table 4 shows that the elasticity modulus significantly decreases when the hydraulic pressure increases from 0 MPa to 1 MPa, thereby highlighting the significant effect of hydraulic pressure on elasticity modulus. The elasticity modulus slightly decreases when the hydraulic pressure further increases from 4 MPa to 7 MPa, thereby suggesting that the influences of hydraulic pressure on elasticity modulus weaken along with the continuous increase in hydraulic pressure.

We hypothesize that the elasticity modulus of sandstone continuously changes in response to the confining pressure ( $\sigma_3$ ). Based on the variation trend of the curves, a regression analysis on elasticity modulus of sandstone under different confining and hydraulic pressures was performed based on the logarithmic function. The data in Table 4 are fitted to obtain the results presented in Fig. 6. The fitting expression is

$$E(\sigma_3) = a \ln E(\sigma_3) + b \quad (8)$$

where  $E(\sigma_3)$  is the elasticity modulus when the hydraulic pressure is  $\sigma_3$ ,  $\sigma_3$  is the confining pressure, and  $a$  and  $b$  are regression coefficients. According to the fitting results, the fitting correlation coefficients exceed 0.94, thereby suggesting a relatively ideal fitting effect.

When the hydraulic pressure is 0 MPa, the fitting formula and correlation coefficient are

$$E(\sigma_3) = 2.06 \ln(\sigma_3) + 9.85367 \quad R^2=0.98691 \quad (9)$$

When the hydraulic pressure is 1 MPa, the fitting formula and correlation coefficient are

$$E(\sigma_3) = 1.82 \ln(\sigma_3) + 9.70945 \quad R^2=0.9406 \quad (10)$$

When the hydraulic pressure is 4 MPa, the fitting formula and correlation coefficient are

$$E(\sigma_3) = 1.82 \ln(\sigma_3) + 8.94357 \quad R^2=0.96489 \quad (11)$$

When the hydraulic pressure is 7 MPa, the fitting formula and correlation coefficient are

$$E(\sigma_3) = 2.54 \ln(\sigma_3) + 5.19981 \quad R^2=0.99596 \quad (12)$$

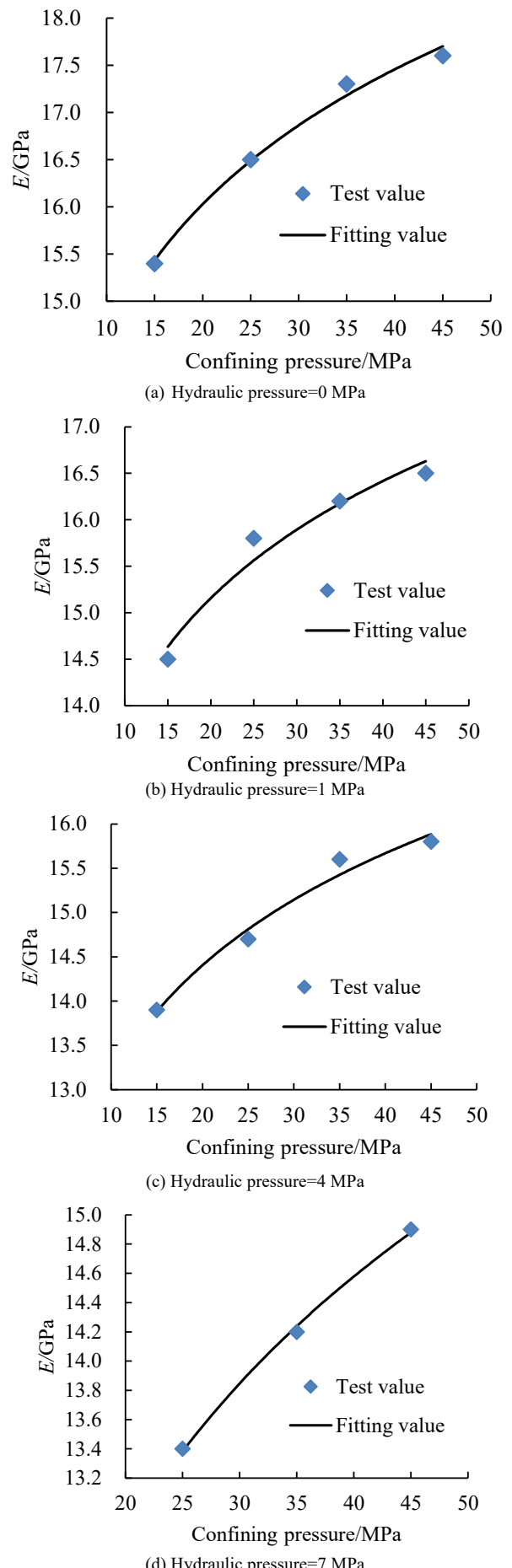


**Fig. 6.** Relation curves between the elasticity modulus ( $E$ ) of sandstones and confining pressure under different hydraulic pressures

The elasticity modulus of sandstone is hypothesized to continuously change in response to hydraulic pressure ( $p$ ). Based on the variation trend of the curves, a regression analysis on the elasticity modulus of sandstone under different confining and hydraulic pressures was performed by using the logarithmic function. The data in Table 4 are fitted to obtain the results presented in Fig. 7. The fitting expression is

$$E(p) = E_0 [1 - a \ln(p + 1)], \quad (13)$$

where  $E(p)$  is the elasticity modulus when the hydraulic pressure is  $p$ ,  $E_0$  is the elasticity modulus under the hydraulic pressure of 0 MPa, and  $a$  is the regression coefficient. The fitting results show that the fitting correlation coefficients exceed 0.93, thereby indicating relatively ideal fitting effects.

When the confining pressure is 15 MPa, the fitting formula and correlation coefficient are

$$E(p) = 15.4 [1 - 0.06424 \ln(p + 1)] \quad R^2 = 0.95227 \quad (14)$$

When the confining pressure is 25 MPa, the fitting formula and correlation coefficient are

$$E(p) = 16.5 [1 - 0.08055 \ln(p + 1)] \quad R^2 = 0.94964 \quad (15)$$

When the confining pressure is 35 MPa, the fitting formula and correlation coefficient are

$$E(p) = 17.3 [1 - 0.07774 \ln(p + 1)] \quad R^2 = 0.93291 \quad (16)$$

When the confining pressure is 45 MPa, the fitting formula and correlation coefficient are

$$E(p) = 17.6 [1 - 0.07126 \ln(p + 1)] \quad R^2 = 0.97194 \quad (17)$$

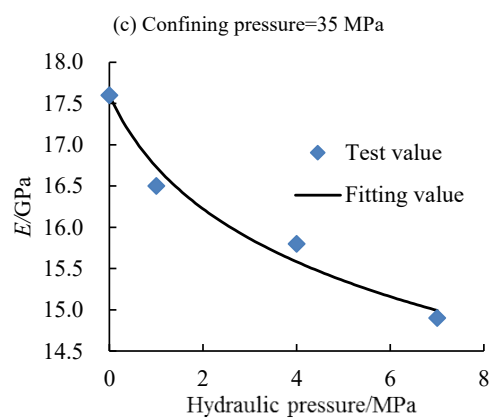
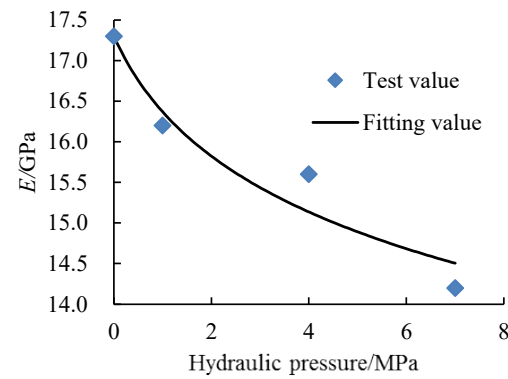
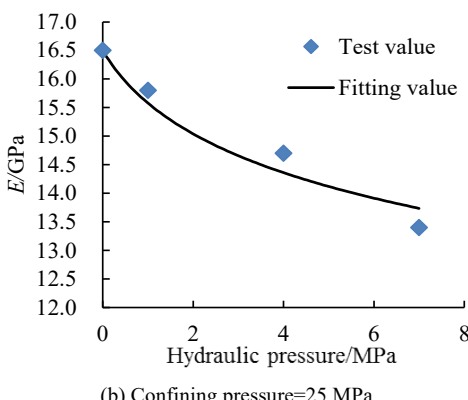
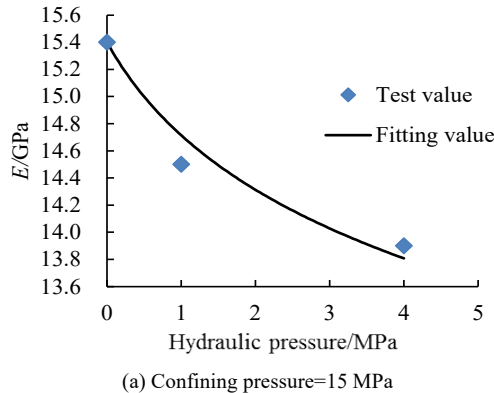


Fig. 7. Relation curves between the elasticity modulus ( $E$ ) of sandstones and hydraulic pressure ( $p$ ) under different confining pressures

The relationships of the elasticity modulus of sandstone with confining and hydraulic pressures are then examined. The test data in Table 4 are fitted to obtain the following binary functional relationship:

$$E = a \ln(\sigma_3) \ln(p + 1) + b \ln(p + 1) + c \ln(\sigma_3) + d \quad (18)$$

where  $E$  is the elasticity modulus under different confining and hydraulic pressures,  $p$  is the hydraulic pressure,  $\sigma_3$  is the confining pressure, and  $a$ ,  $b$ , and  $c$  are the regression coefficients. The fitting surface is shown in Fig. 8, where  $a = -0.1681$ ,  $b = -0.6952$ ,  $c = 2.02$ ,  $d = 9.998$ , and  $R^2 = 0.9544$ . In sum, the functional relationships of the elasticity modulus of sandstone with confining and hydraulic pressures are reasonable. Moreover, the changes in the elasticity modulus under different confining and hydraulic pressures can be predicted based on  $\sigma_3$  and  $p$  in these binary functions.

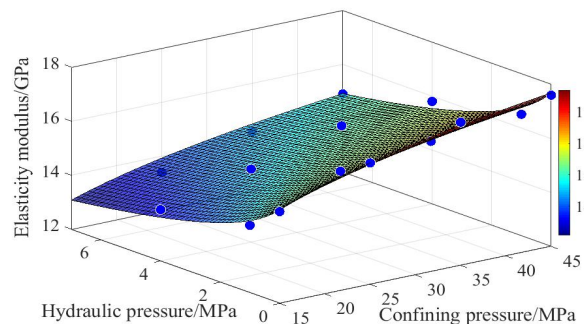


Fig. 8. Relationships of elasticity modulus with hydraulic ( $P$ ) and confining pressures ( $\sigma_3$ )

## (2) Change characteristics of axial peak strain

Peak strain can be directly obtained from the stress-strain test results. The changes in the axial peak strain of sandstone with confining and hydraulic pressures are listed in Table 5.

**Table 5.** Axial peak strain of sandstone under different confining and hydraulic pressures

Confining pressure /MPa	Peak strain of sandstone/%			
	Hydraulic pressure 0 MPa	Hydraulic pressure 1 MPa	Hydraulic pressure 4 MPa	Hydraulic pressure 7 MPa
15	0.8976	0.85760	0.792089	--
25	1.0220	0.97011	0.945555	0.859813
35	1.2907	1.18579	1.051024	1.037108
45	1.3623	1.23203	1.120722	1.052798

Given the same hydraulic pressure, the axial peak strain linearly increases along with confining pressure because the sandstone shifts from the brittle state to the ductile state as the confining pressure increases. Under the same confining pressure, the axial strain gradually decreases along with an increasing hydraulic pressure. In other words, increasing the hydraulic pressure also increases the chances for the sandstone to develop brittle failure. Given that the variation law of axial peak strain is similar to that of compressive strength, the binary functional relationships of axial peak strain (Table 5) with the confining and hydraulic pressures are fitted. The fitting relation is

$$\varepsilon_c = a\sigma_3 \ln(p+1) + b \ln(p+1) + c\sigma_3 + d \quad (19)$$

where  $\varepsilon_c$  is the axial peak strain under different confining and hydraulic pressures,  $p$  is the hydraulic pressure,  $\sigma_3$  is the confining pressure, and  $a$ ,  $b$ , and  $c$  are the regression coefficients. The fitting surface is shown in Fig. 9, where  $a=-0.003279$ ,  $b=-0.000716$ ,  $c=0.01624$ ,  $d=0.6507$ , and  $R^2=0.9537$ . In a word, the functional relations of the axial peak strain of sandstone with the confining and hydraulic pressures are reasonable. Moreover, the changes in the axial peak strain under different confining and hydraulic pressures can be predicted based on  $\sigma_3$  and  $p$  in these binary functions.

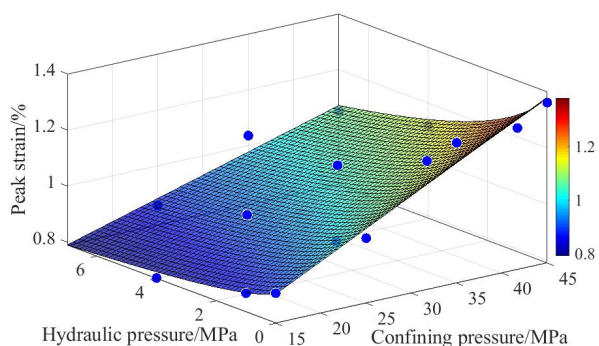


**Fig. 9.** Relationships of axial peak strain with hydraulic ( $P$ ) and confining pressures ( $\sigma_3$ )

## 5. Conclusions

A triaxial loading test of sandstone under high stress and high hydraulic pressure is performed in this study. The findings of this work can provide some references for the excavation of deep underground tunnels under high hydraulic pressure. The following major conclusions are drawn from this work:

(1) The influences of hydraulic pressure on the strength of sandstone are gradually weakened. As the hydraulic pressure increases, sandstones become filled with water, thereby resulting in stable influences. The strength of the sandstones rapidly decreases in the early stress-strain stage.

(2) Under high stress, the compressive strength of sandstones under different initial confining pressures decreases in the logarithmic function pattern along with an increasing hydraulic pressure ( $p$ ).

(3) Under different hydraulic pressures, a regression analysis on the changes of elasticity modulus of sandstone with the confining pressure ( $\sigma_3$ ) is performed by using a logarithmic function. Under different confining pressures, the elasticity modulus shows a decreasing trend in its logarithmic function pattern as the hydraulic pressure increases.

(4) Given the same hydraulic pressure, the axial peak strain linearly increases along with confining pressure, and the sandstone shifts from the brittle state to the ductile state accordingly. Under the same confining pressure, the axial strain gradually decreases along with an increasing hydraulic pressure, thereby suggesting that increasing the hydraulic pressure will increase the chances for sandstone to develop brittle failures.

The mechanical properties of sandstone as obtained from the triaxial test offer some references for the construction of underground projects under high hydraulic pressures and for studying the variation laws of the strength and deformation parameters of rock masses at various depths under different hydraulic pressures. However, given the space limitations, this study did not perform an unloading triaxial test under high stress and high hydraulic pressures. The excavation of underground tunnels is mainly in the unloading stress state. In the future, the authors plan to perform an unloading triaxial experimental study under high stress and high hydraulic pressure.

## Acknowledgments

This study was supported by the National Key R&D Program of China (2018YFC1504802), the Fundamental Research Funds for the Central Universities (Project No. 2019CDCG0013), and Scientific Innovation Research of Chongqing Scientific Department (Project No. cstc2017shms-zdyf0412).

This is an Open Access article distributed under the terms of the Creative Commons Attribution License



## References

- Diering, D. H., "Tunnels under pressure in an ultra-deep Witwatersrand gold mine". *Journal of the South African Institute of Mining and Metallurgy*, 100(6), 2000, pp.319-324.

2. Vogel, M., Rast, H. P., "AlpTransit-safety in construction as a challenge: health and safety aspects in very deep tunnel construction". *Tunnelling & Underground Space Technology*, 15(4), 2000, pp.481-484.
3. Gurtunca, R. G., Keynote, L., "Mining below 3000m and challenges for the South African gold mining industry". *Proceedings of Mechanics of Jointed and Fractured Rock*, 66, 1998, pp.3-10.
4. Yang, S. Q. , Jing, H. W. , Cheng, L., "Influences of pore pressure on short-term and creep mechanical behavior of red sandstone". *Engineering Geology*, 179, 2014, pp.10-23.
5. Alam, A. K. M. B., Niioka, M., Fujii, Y., et al. "Effects of confining pressure on the permeability of three rock types under compression". *International Journal of Rock Mechanics & Mining Sciences*, 65(1), 2014, pp.49-61.
6. Hokka, M., Black, J., Tkalich, D., et al. "Effects of strain rate and confining pressure on the compressive behavior of Kuru granite". *International Journal of Impact Engineering*, 91, 2016, pp.183-193.
7. Liang C., Wu, S., Li, X., et al. "Effects of strain rate on fracture characteristics and mesoscopic failure mechanisms of granite". *International Journal of Rock Mechanics and Mining Sciences*, 76, 2015, pp.146-154.
8. Tkalich, D., Fourneau, M., Kane, A., et al. "Experimental and numerical study of Kuru granite under confined compression and indentation". *International Journal of Rock Mechanics and Mining Sciences*, 87, 2016, pp.55-68.
9. Yuya, Sakai., Massao, Nakatani., Akihiro, Takeuchi,, et al. "Mechanical behavior of cement paste and alterations of hydrates under high-pressure triaxial testing". *Journal of Advanced Concrete Technology*, 14, 2016, pp.1-12.
10. Abdallah, A., Laurent, D., Yann, M.. "Investigation of the Interstitial Pore Pressure of Saturated Concrete under High Confinement". *Proceedings*, 2, 2018, pp.1-5.
11. Piotrowska, E., Forquin, P., Malecot, Y., "Experimental study of static and dynamic behavior of concrete under high confinement: Effect of coarse aggregate strength". *Mechanics of Materials*, 92, 2016, pp.164-174.
12. Zhao, Y., Tang, J., Chen, Y., et al. "Hydromechanical coupling tests for mechanical and permeability characteristics of fractured limestone in complete stress-strain process". *Environmental Earth Sciences*, 76(1), 2017, pp.24-31.
13. Li, Y., Chen, Y. F., Zhou, C. B., "Effective Stress Principle for Partially Saturated Rock Fractures". *Rock Mechanics and Rock Engineering*, 49(3), 2016, pp.1091-1096.
14. Chernak, L. J., Hirth, G., "Deformation of antigorite serpentinite at high temperature and pressure". *Earth and Planetary Science Letters*, 296, 2010, pp.0-33.
15. Mohamadi, M., Wan, R. G., "Strength and post-peak response of Colorado shale at high pressure and temperature". *International Journal of Rock Mechanics and Mining Sciences*, 84, 2016, pp.34-46.
16. Ding, Q. L., Ju, F., Song, S. B., et al. "An experimental study of fractured sandstone permeability after high-temperature treatment under different confining pressures". *Journal of Natural Gas Science and Engineering*, 34, 2016, pp.55-63.
17. Liu, S., Xu, J., "Effect of strain rate on the dynamic compressive mechanical behaviors of rock material subjected to high temperatures". *Mechanics of Materials*, 82, 2015, pp.28-38.
18. Ding, Q. L., Ju, F., Mao, X. B., et al. "Experimental Investigation of the Mechanical Behavior in Unloading Conditions of Sandstone After High-Temperature Treatment". *Rock Mechanics and Rock Engineering*, 49(7), 2016, pp.2641-2653.
19. Jiang, H. F., Liu, D. Y., Huang, W., et al. "Influence of high pore water pressure on creep properties of rock under high confining pressure". *Journal of China Coal Society*, 39(7), 2014, pp.1248-1256.